Effect of aging heat treatment on the microstructure and hardness of a serviced ZHS32 superalloy

Mohammad Shademani, Ali Sedaghat Ahangari Hossein Zadeh ✉, Mohammad Reza Rahimipour, Mohammad Farvizi

Department of Ceramics, Materials and Energy Research Center (MERC), Karaj, P.O. Box 31787-316, Iran
✉ *E-mail: a.sedaghat@merc.ac.ir*

Published in Micro & Nano Letters; Received on 2nd December 2017; Revised on 3rd October 2018; Accepted on 22nd October 2018

According to the gradual changes of the microstructure of superalloys during harsh service condition of turbine blades and the detrimental effects of these changes on the mechanical properties of superalloys, performing of a rejuvenation heat treatment (solution treatment + aging process) on ex-serviced superalloys is necessary. In this work, the aging heat treatment was conducted on a serviced single crystal ZHS32 superalloy in the temperature range of 950–1150°C. It was found that while performing the aging process at 950 and 1050°C for 10 h did not provide appropriate conditions for the nucleation and growth of primary ϒ′ phases, conducting aging at the temperature of 1150°C for 10 and 16 h yields to the formation of ϒ′ precipitates with the desired cuboidal morphology. The comparison of the microstructure of the rejuvenated samples with the un-rejuvenated samples confirms that with applying this procedure, the size of strengthening ϒ′ precipitates reduces and the volume fraction of these phases considerably increases, which yields to the recovery of the superalloy microstructure and improvement of its mechanical properties such as hardness.

1. Introduction: Superalloys are high-performance alloys that have several key properties such as excellent mechanical strength, creep resistance, good surface stability, and corrosion and oxidation resistance [1, 2]. Recently, nickel-based superalloys are used on a large scale in various industries such as gas turbine blades in power plants and jet engines. The shape of these blades and their ability to withstand corrosion and high temperature are effective in the final efficiency of the gas turbine [3–5]. The dominant mechanism of degradation in nickel-based superalloys is the occurrence of the creep phenomenon in grain boundaries. As a result, the directionally solidified superalloys and, ultimately, single crystal superalloys were developed to overcome this problem [6]. Controlling the morphology is regarded as one of the advantages of nickel-based superalloys which results in improving mechanical properties. The main phases in the nickel-based superalloys are **ϒ** matrix, ϒ′ phase, and carbides. The ϒ phase is a solid solution with fcc crystal structure in which elements such as chromium, cobalt, iron, molybdenum, and tungsten result in strengthening the solution [7]. The ϒ′ phase is very important as it is the main factor of high-temperature stability. This phase has an $L1_2$ crystal structure and its chemical composition is Ni_3X. X can be electropositive elements such as Al and Ti [1]. The mentioned phase is a precipitation hardening agent in nickel-based superalloys. Generally, in Ni-based superalloys, two types of ϒ′ precipitates can be formed: (i) primary ϒ′ with cuboid morphology and (ii) secondary ϒ′ precipitates with spherical morphology. In a typical Ni-based superalloy, fine and homogeneously dispersed secondary ϒ′ precipitates provide creep resistance while coarse primary ϒ′ precipitates improve the ductility of the alloy. As a consequence, a bimodal configuration of primary and secondary gamma prime precipitates is favoured. [8]. On the other hand, the conventional carbides in nickel-based superalloys include $M_{23}C_6$, M_6C and MC in which M represents an active or refractory element [9]. During operation of turbine blades, the microstructure of underlying superalloys gradually changes which is regarded as one of the reasons for the loss of mechanical properties of superalloys during the use of turbine blades. The high cost of replacing these parts during breakdown has led to an interest in extending blade service life through operations such as turbine blade rejuvenation in the industry. This operation should be timely applied to prevent the occurrence of failures and heavy damages [10, 11]. The most important changes in the microstructure of superalloys can be summarised as follows:

- The change in the morphology of primary ϒ′ precipitates from initial cubic state to irregular shapes and rafting, which deteriorates mechanical properties, such as creep resistance.
- ϒ′ precipitates growth.
- The precipitation of continuous carbides on grains boundaries.
- The precipitation of harmful phases such as TCP.
- The reduction of volume percentage of the ϒ′ precipitates [1].

Generally, any method which improves the service life of the components is known as ‘rejuvenation’. Heat treatment is one of the methods of rejuvenation which includes solution treatment (ST) and aging process. During ST, the precipitated phases including ϒ′, TCP and carbide phases (other than hardly soluble MC carbides) are mainly dissolved at a temperature higher than the temperature of the ϒ′ phase dissolution in the matrix of **ϒ** resulting in creating a homogeneous structure. Then, new ϒ′ phases are precipitated and grow with the desired cuboidal morphology in the second stage (aging process) [1, 4].

ZHS32 is a single-crystal Ni-based superalloy which contains a series of alloy elements (Al, Cr, Co, Mo, W, Ta, Nb). It is currently used in new generation turbine blades [12]. In this superalloy, 4 wt% of rhenium element is added to improve its creep strength. Various aspects of this superalloy such as its thermal fatigue and creep behaviour [13], microstructural investigation of ZHS32 after selective laser melting, vacuum heat treatment and hot isostatic pressing [14], and the influence of heat treatment on the composition of carbide phases [15] have been investigated.

In our previous study [16], we have determined the ST conditions of a serviced ZHS32 turbine blade. In this Letter, the influence of different aging conditions on the microstructure and hardness of a serviced ZHS32 superalloy will be investigated.

doi: 10.1049/mnl.2018.5092

2. Experimental activities: In this Letter, an ex-serviced ZHS32 superalloy was employed. The as-received ZHS32 superalloy was subjected to a standard heat treatment including ST at 1270°C for 3 h, followed by water quenching with a 200°C/s cooling rate, and the aging process at 1050°C for 10 h [17]. The chemical composition of this alloy is presented in Table 1. Samples with 1×1 cm^2 dimension were prepared by the wire cut method from the central part of the blade which had the highest destruction in the structure.

After preparing the small-sized samples, their diffusion coatings were first stripped based on the following procedure, according to the U.S. Patent No. 4,339,282:

- Removing the oxide layer by sand blasting (60 and 80).
- Removing the diffusion coating by chemical method.
- Ensuring a complete removal of the coating by placing samples in the furnace at 540°C for 1 h and detecting the successful removal of the coating by the surface colour of the samples (blue).

It should be noted that the process of determining the parameters of the ST was conducted in an independent research based on microscopic observations (SEM images) [16] in which the suitable temperature for ST was obtained to be 1350°C for 3 h and then,

Table 1 Chemical composition of ZHS32 superalloy (wt%)

C	0.15	W	8.50	Nb	1.87
Cr	5.09	Mo	1.29	Hf	0.03
Co	9.27	Ti	0.06	Re	4
Ta	4.01	Al	5.86	Ni	Bal.

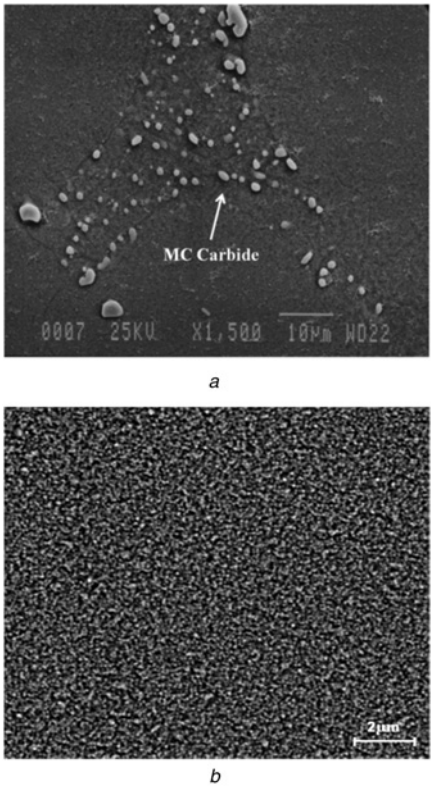

Fig. 1 *SEM image of the microstructure after ST at 1350°C for 3 h and water quenching*
a Low magnification [16] and
b High magnification

Table 2 Aging heat treatment conditions

	Maintaining time, h	Aging temperature, °C	Cooling environment
1	10	950	air
2	10	1050	
3	10	1150	
4	16	1150	

solution treated samples were water quenched from peak temperature to room temperature at a cooling rate of about 200°C/s. Figs. 1*a* and *b* represent the microstructure of this superalloy after ST. Based on Fig. 1, the microstructure is free from primary ϒ′ precipitates with cubic morphology and only supercooling ϒ′ precipitates exist in the microstructure. The solution treated samples were subjected to aging treatment according to condition presented in Table 2. The optimal temperature and time of aging were determined by the evaluation of the microstructure with SEM images.

In order to investigate the microstructure of samples, a scanning electron microscope (VEGA\TESCAN-LMU) was used. The volume fraction of phases and the size of precipitates in the microstructure were determined by Clemex software.

The hardness of the samples was evaluated before and after heat treatment by Vickers Hardness Test (MVK H21-Akashi Japan) based on the standard of ASTM-C13227-08 (under the load of 10 kg). In this method, the hardness of samples was calculated using (1) in MPa [18]

$$H_V = 1.854 \frac{F}{D^2} \tag{1}$$

where H_V indicates the Vickers hardness, F represents the applied load in kilogram (kg), and D shows the average diameters of the created effect in millimetres (mm). In order to improve the accuracy of the test, the test was repeated five times for each sample, and the average of the obtained values was reported.

3. Results and discussion

3.1. Effect of aging heat treatment on the microstructure:: Selection of an appropriate aging condition can lead to the formation of a microstructure with desired ϒ′ size, cuboidal morphology and good distribution [1]. Fig. 2 indicates the microstructure of the solution treated sample at 1350°C for 3 h and aged at 950°C for 10 h. The precipitation of the ϒ′ phase during the aging process occurs when the thermodynamic and kinetic conditions are both provided. Thus, a decrease in the temperature makes the mobility of atoms and their diffusion more difficult as one of the most important kinetic conditions, although the temperature reduction is necessary to provide the thermodynamic conditions of transformation. Therefore, a temperature is suitable for aging operation in which the primary ϒ′ phases can precipitate at this temperature. During the aging process, the ϒ′ precipitates grow with emitting the dissolved elements such as Al and Ta from the supersaturated solid solution and their adherence to the precipitates [1]. As shown in Fig. 2, the primary ϒ′ precipitates with the desired cuboidal morphology have not yet germinated, which indicates that the temperature of 950°C and 10 h does not provide the necessary activation energy for the diffusion and growth of ϒ′ precipitates. Therefore, the microstructure of this superalloy at this condition consists of ϒ′ precipitates at the nanoscale with spherical morphology. The reason for the sphericity of these precipitates is that in the early stages of aging, the system selects a spherical shape with the lowest surface-to-volume ratio to reduce the interface energy [19].

Fig. 3 shows the microstructure of the sample after ST at 1350°C for 3 h and aging at 1050°C for 10 h. As observed, there are still super-cooling ϒ′ precipitates in the microstructure, which have not yet grown, and the cubic ϒ′ particles resulted from the aging

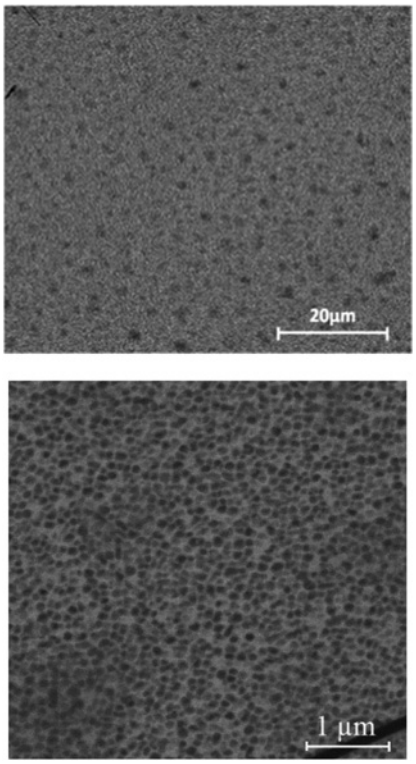

Fig. 2 *Microstructure of solution treated samples at 1350°C for 3 h and aged at 950°C for 10 h with different magnifications*

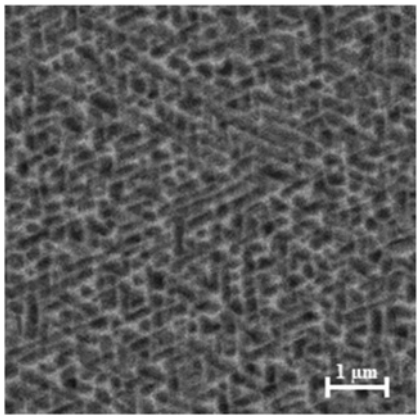

Fig. 3 *Microstructure of solution treated samples at 1350°C for 3 h and aged at 1050°C for 10 h*

operations have not been precipitated in the structure. Based on this observation, the temperature of 1050°C is not sufficient for particle growth and precipitation of primary ϒ′ particles.

As shown in Figs. 4 and 5, after aging heat treatment at 1150°C for 10 and 16 h, the ϒ′ precipitates evolved with regular and cubic morphology, similar to the ϒ′ morphology of this superalloy before service. The kinetics of ϒ′ particles growth in **ϒ** matrix has been studied in Ni-based superalloy [19]. At the initial stages of the aging process, very small nuclei of ϒ′ phase uniformly nucleate in **ϒ** matrix. After growth of these small precipitates, the larger particles absorb the smaller particles through volumetric diffusion. The reduction of interface energy is the main driving force of this process (Ostwald ripening process). Finally, small particles disappeared during aging heat treatment and the size of larger particles increased [19]. By comparing the microstructure of ϒ′ after the aging heat treatment at 1150°C for different time periods (10 and

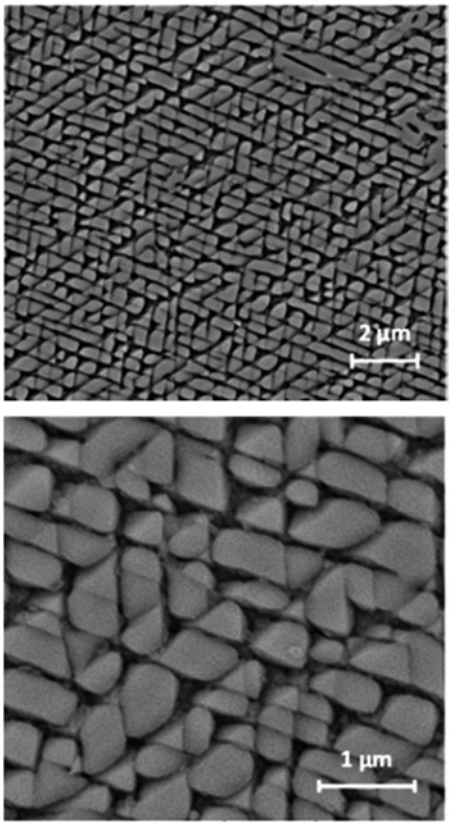

Fig. 4 *Microstructure of the ZHS32 superalloy after ST at 1350°C for 3 h and aging at 1150°C for 10 h with different magnifications*

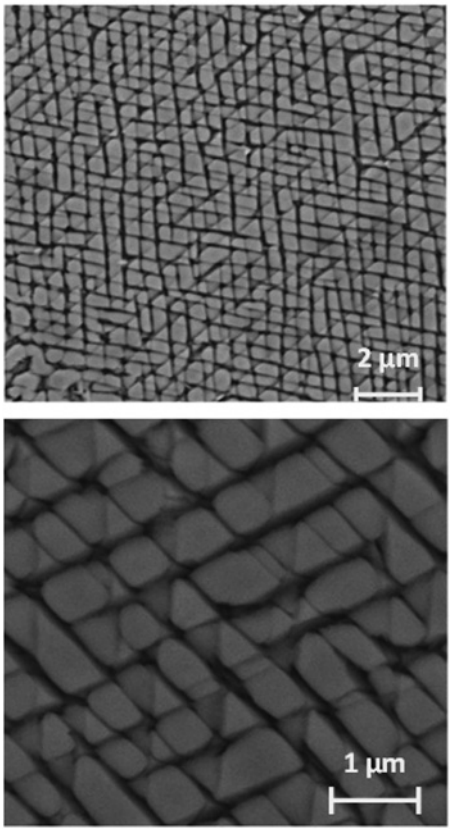

Fig. 5 *Microstructure of the ZHS32 superalloy after ST at 1350°C for 3 h and aging at 1150°C for 16 h with different magnifications*

doi: 10.1049/mnl.2018.5092

16 h), it is concluded that the ϒ′ particles have a higher order and uniform size and the gap between the particles is reduced after aging at 1150°C for 16 h. It is well-known that the formation of a fine array of ϒ′ precipitates can considerably improve the mechanical properties of the superalloy [16]. Based on the fact that an increase in the aging temperature of the ϒ′ particles enhances the diameter of ϒ′ particles (the particles become bigger), the first aging temperature and time in which the appropriate volume fraction of fine ϒ′ particles with the desired morphology created, is selected as the aging conditions.

Fig. 6*a* illustrates the microstructure of ZHS32 superalloy before degradation with 100 h service which mainly consists of primary ϒ′ precipitates. Also, secondary ϒ′ phases with spherical morphology can be detected in the microstructure. Fig. 6*b* depicts the microstructure of superalloy after 700 h service and before the rejuvenation process in which ϒ′ precipitates have irregularly rafted morphology. However, after a rejuvenation process on this sample (ST at 1350°C for 3 h followed by water quenching with 200°C/s cooling rate and aging at 1150°C for 10 h) (Fig. 6*c*); a regular and cubic morphology of ϒ′ has evolved. It is expected that after restoring the microstructure by the rejuvenation heat treatment, the remaining life of these blades will increase due to the microstructure recovery.

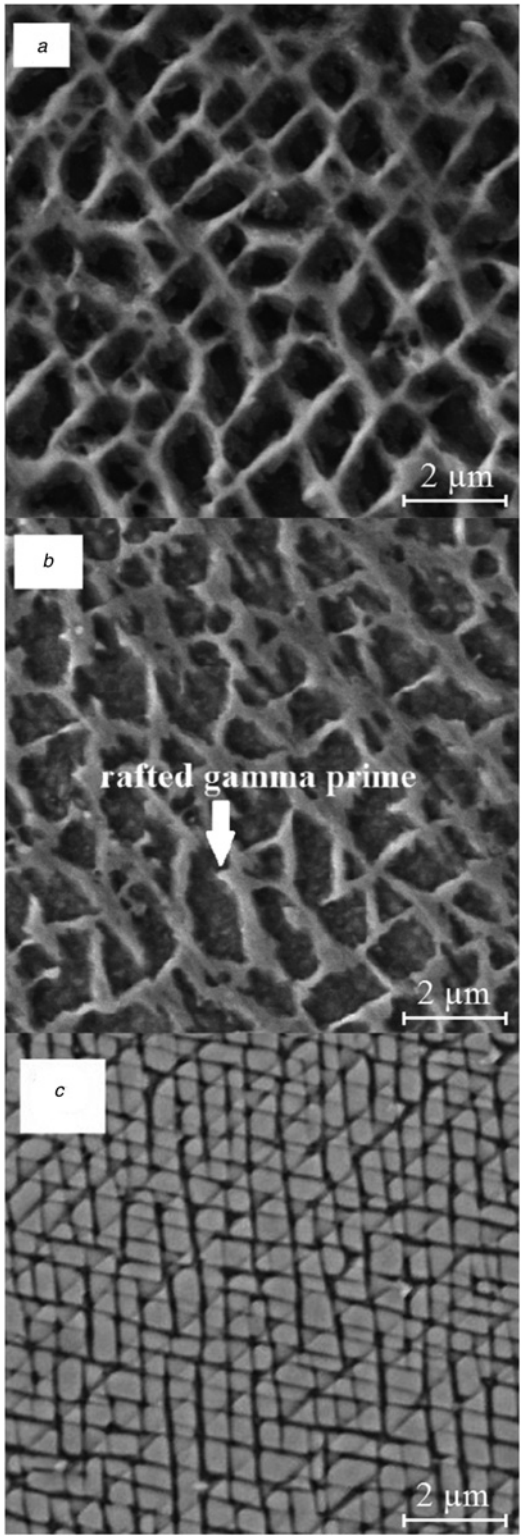

Fig. 6 *SEM micrographs of a ZHS32 superalloy, after*
a 100 h service
b 700 h service
c Rejuvenation process (solution treatment at 1350°C for 3 h followed by water quenching with a 200°C/s cooling rate and aging at 1150°C for 10 h)

3.2. Effect of aging heat treatment on the volume fraction and the size of ϒ′ precipitates: The results of measurement of ϒ′ volume fraction and particle size before and after rejuvenation are summarised in Fig. 7 and Table 3. It is seen that the size of ϒ′ precipitates during service at high temperature increases. Furthermore, the volume percentage of these precipitates reduces and rafting occurs in ϒ′ precipitates. Formation of rafted ϒ′ phases caused the dislocations to easily pass through precipitates and, as a result, a decrease takes place in the mechanical properties such as creep resistance. The results of measurements of ϒ′ precipitates after rejuvenation show that by performing rejuvenation heat treatment (ST at 1350°C for 3 h and aging at 1150°C for 10 h), the size of ϒ′ precipitates significantly decreased while the volume fraction of these precipitates increased. According to Table 3, an increase in the aging time from 10 to 16 h increased the average precipitate size from 0.49 ± 0.12 to 0.55 ± 0.09 μm and the volume percentage of ϒ′ precipitates increased from 71 to 75% (Fig. 7).

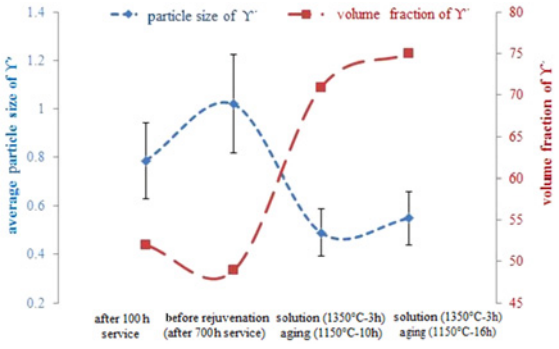

Fig. 7 *Variations of the average size of ϒ′ precipitates and their volume fractions before and after rejuvenation process*

Table 3 Size of ϒ′ precipitates in the microstructure (in microns) before and after ST at 1350°C for 3 h and aging in different conditions

Samples condition	Number of measured precipitates	Min. size	Max. size	Average size
before rejuvenation (after 100 h service)	30	0.455	1.057	0.786
before rejuvenation (after 700 h service)	30	0.49	1.8	1.02
ST + aging at 1150°C – 10 h	30	0.28	0.73	0.49
ST + aging at 1150°C – 16 h	30	0.36	0.75	0.55

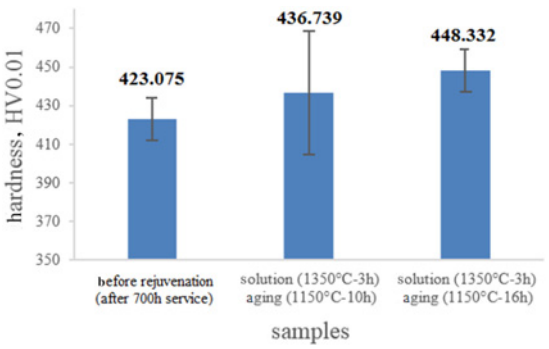

Fig. 8 *Hardness of samples based on the heat treatment conditions*

3.3. Effect of the aging process on the hardness: Fig. 8 indicates the results of the hardness test (Vickers) for the base sample after 700 h service and rejuvenated samples (ST at 1350°C for 3 h followed by water quenching with 200°C/s cooling rate and aging at 1150°C for 10 and 16 h). It is seen that the average hardness for the rejuvenated samples is higher than the average hardness of non-rejuvenated samples. According to the data provided in Fig. 7, after rejuvenation process the volume fraction of ϒ′ precipitates considerably increases and the average precipitate size decreases, which provide more effective barriers against dislocations motion, leading to the improved hardness of the rejuvenated superalloy [20].

4. Conclusion: In this Letter, the influence of aging heat treatment on the microstructure and hardness of a serviced ZHS32 superalloy has been studied. It was found that performing the aging heat treatment at the temperatures of 950 and 1050°C for 10 h on the solution treated samples did not provide an appropriate condition for the nucleation and growth of ϒ′ precipitates. However, with a further increment of aging temperature and performing of the aging process at 1150°C for 10 and 16 h, a fine array of primary ϒ′ phases with a cuboidal morphology formed in the microstructure of superalloy. The measurements of the size and volume fraction of ϒ′ precipitates have shown that with performing of the rejuvenation process (ST at 1350°C for 3 h and aging at 1150°C for 10 and 16 h) the size of the desired ϒ′ phases considerably reduces and the volume fraction of this phase increases. According to the strengthening role of these precipitates, the hardness of rejuvenated samples was higher than that of the samples without the rejuvenation process.

5 References

[1] Sims C., Stoloff N., Hagel W.: 'Superalloys II–high-temperature materials for aerospace and industrial applications' (Wiley, New York, 1987)

[2] Farvizi M., Asgari S.: 'Effects of cold work prior to aging on microstructure of AEREX^{TM}350 superalloy', *Mater. Sci. Eng. A*, 2008, **480**, pp. 434–438

[3] Kablov E., Petrushin N., Bronfin M., *ET AL.*: 'Specific features of rhenium-alloyed single-crystal nickel superalloys', *Russ. Metall. (Metally)*, 2006, **2016**, (5), pp. 406–414

[4] Furrer D., Shankar R., White C.: 'Optimizing the heat treatment of Ni-based superalloy turbine discs', *JOM*, 2003, **55**, (3), pp. 32–34

[5] Kim M., Chang S., Won J.: 'Effect of HIP process on the microstructural evolution of a nickel-based superalloy', *Mater. Sci. Eng. A*, 2006, **441**, (1), pp. 126–134

[6] Baldan A.: 'Rejuvenation procedures to recover creep properties of nickel-base superalloys by heat treatment and hot isostatic pressing techniques', *J. Mater. Sci.*, 1991, **26**, (13), pp. 3409–3421

[7] Padalko A., Avdyukhin S., Veselov A., *ET AL.*: 'Precipitation of the γ′ phase in a nickel alloy under conditions of static barothermal treatment', *Russ. Metall. (Metally)*, 2006, **2006**, (1), pp. 73–79

[8] Hosseini S.S., Nategh S., Ekrami A.-A.: 'Microstructural evolution in damaged IN738LC alloy during various steps of rejuvenation heat treatments', *J. Alloys Compd.*, 2012, **512**, (1), pp. 340–350

[9] Lvov G., Levit V., Kaufman M.: 'Mechanism of primary MC carbide decomposition in Ni-base superalloys', *Metall. Mater. Trans. A*, 2004, **35**, (6), pp. 1669–1679

[10] Han X.: 'Diffusion coatings for high-temperature applications on Ni-base superalloys', 2012

[11] Wangyao P., Lothongkum G., Krongtong V., *ET AL.*: 'Effect of heat treatments after HIP process on microstructure refurbishment in cast nickel base superalloy', *IN-738. J. Met. Mater. Miner.*, 2005, **15**, (2), pp. 69–78

[12] Kishkin S.T., Kablov E.N.: 'Cast high-temperature superalloys for turbine blades', in aviatsionnye materialy' (MISiS–VIAM, Moscow, 2002), pp. 48–58

[13] Getsov L.B., Semenov A.S., Semenov S.G., *ET AL.*: 'Experiments and failure criteria for single crystal alloys of gas turbine engine under static and thermocyclic loading'. Available at http://www.icas.org/ICAS_ARCHIVE/ICAS2014/data/papers/2014_0569_paper.pdf, September 2014

[14] Zavodov A.V., Petrushin N.V., Zaitsev D.V.: 'Microstructure and phase composition of ZHS32 superalloy after selective laser melting, vacuum heat treatment and hot isostatic pressing', *Lett. Mater.*, 2017, **7**, (2), pp. 111–116

[15] Pigrova G.D., Rybnikov A.I.: 'Carbidephases in a multicomponent superalloy Ni-Co-W-Cr-Ta-Re', *Phys. Met. Metallogr.*, 2013, **114**, (7), pp. 593–595

[16] Shademani M., Rahimipour M.R., Sedaghat A., *ET AL.*: 'Determination of solution temperature in an ex-service Ni-based turbine blade', *J. Adv. Mater. Process.*, 2017, **4**, (3), pp. 66–72

[17] Protasova N.A., Svetlov I.L., Bronfin M.B., *ET AL.*: 'Lattice-parameter misfits between the γ and γ′ phases in single crystals of nickel superalloys', *Phys. Metals Metallogr.*, 2008, **106**, (5), pp. 512–519

[18] Dieter G.E., Bacon D.J.: 'Mechanical metallurgy', vol. 3 (McGraw-Hill, New York, 1986)

[19] Zhang J., Singer R.: 'Hot tearing of nickel-based superalloys during directional solidification', *Acta Mater.*, 2002, **50**, (7), pp. 1869–1879

[20] Guo Z.L., Saunders N., Miodownik A.P., *ET AL.*: 'Quantification of high temperature strength of nickel-based superalloys', *Mater. Sci. Forum*, 2007, **546-549**, pp. 1319–1326

doi: 10.1049/mnl.2018.5092